Research Article

Mediterranean Marine Science
Indexed in WoS (Web of Science, ISI Thomson) and SCOPUS
The journal is available on line at http://www.medit-mar-sc.net
DOI: http://dx.doi.org/10.12681/mms.22932

High proliferation of *Pseudo-nitzschia* cf. *arenysensis* in the Adriatic Sea: ecological and morphological characterisation

Jasna ARAPOV[1], Mia BUŽANČIĆ[1], Antonella PENNA[1,2,3], Silvia CASABIANCA[2,3], Samuela CAPELLACCI[2,3], Francesca ANDREONI[2], Sanda SKEJIĆ[1], Ana BAKRAČ[1], Maja STRAKA[1], Jelena MANDIĆ[1] and Živana Ninčević GLADAN[1]

[1] Institute of Oceanography and Fisheries, Laboratory of Plankton and Shellfish Toxicity, Šetalište I. Meštrovića 63, 21000 Split, Croatia
[2] University of Urbino, Department of Biomolecular Sciences, Campus E. Mattei, 61029 Urbino, Italy
[3] CoNISMa, National Inter-University Consortium for Marine Sciences, 00196 Roma, Italy
[4] IRBIM CNR, Institute for Biological Resources and Marine Biotechnology, 60125 Ancona, Italy

Corresponding author: arapov@izor.hr

Handling Editor: Yelda AKTAN

Received: 14 April 2020; Accepted: 22 October 2020; Published online: 1 December 2020

Abstract

The aim of this study is to characterise the diatom *Pseudo-nitzschia* community during a bloom period in relation to environmental conditions. High proliferation of *Pseudo-nitzschia* spp. was observed in September 2017 at the shellfish breeding area in Krka River estuary (Central eastern Adriatic Sea). The peak of abundance (1.8 x 10^6 cells L^{-1}) was recorded at 7 m depth, and the increased abundance persisted for four weeks. Morphological analyses of field samples based on scanning electron microscopy (SEM) revealed that *Pseudo-nitzschia* cf. *arenysensis* prevailed (94%) in the *Pseudo-nitzschia* assemblage. Several strains were successfully isolated from net samples in order to better define morphological features and phylogenetic characterisation. The isolated *Pseudo-nitzschia* strains corresponded morphologically to *P.* cf. *arenysensis* from the field samples, based on our SEM observations. Phylogenetic analysis demonstrated that the Croatian strains grouped with *P. arenysensis* using the ITS and LSU rDNA sequences.

The Spearman rank correlation showed that salinity was an important environmental factor affecting the vertical distribution of *Pseudo-nitzschia* spp. in this highly variable area. Availability of increased concentration of orthophosphates and ammonium and a low Si:TIN ratio may have promoted the bloom of *P.* cf. *arenysensis* in the estuary.

Keywords: Adriatic Sea; *Pseudo-nitzschia* bloom; SEM; ribosomal genes.

Introduction

To date, the genus of marine diatoms *Pseudo-nitzschia* H. Pergallo consists of 54 described species (Bates *et al*., 2018; Huang *et al*., 2019). *Pseudo-nitzschia* species are distributed worldwide, from tropical to polar areas (Lelong *et al*., 2012; Trainer *et al*., 2012; Bates *et al*., 2018). This genus received significant attention from the scientific community after 1987, when the first ASP (Amnesic Shellfish Poisoning) outbreak was caused by a bloom of *P. multiseries* Hasle (Hasle) (Wright *et al*., 1989). Since then, the number of toxic *Pseudo-nitzschia* species that produce domoic acid (DA) increased to 26 (Bates *et al*., 2018; Lundholm, 2019). Domoic acid is a potent neurotoxin, found in various marine organisms such as zooplankton, shellfish, crustaceans, echinoderms, worms, marine mammals and birds, which can cause severe human intoxication and harmful impact on marine wildlife (Trainer *et al*., 2012; La Barre *et al.,* 2014). The genus *Pseudo-nitzschia* is a common member of the phytoplankton community in the Adriatic Sea (Viličić *et al*., 2007; Bužančić *et al*., 2012; Marić *et al*., 2012; Skejić *et al*., 2014; Ninčević Gladan *et al.* 2020; Turk Dermastia *et al.* 2020). Previous taxonomical studies of *Pseudo-nitzschia* diversity from the central part of the Eastern Adriatic coast were mainly based on morphological data and included reports on species, such as: *P. pseudodelicatissima*, *P. delicatissima*, *P. subfraudulenta*, *P. calliantha*, *P. fraudulenta*, *P. pungens*, *P. mannii* (Burić *et al*., 2008; Marić Pfannkuchen, 2013; Arapov *et al*., 2016; Arapov *et al*., 2017). A phylogenetic description of Croatian *Pseudo-nitzschia* spp. was found only in the study of *P. mannii* (Grbin *et al*., 2017).

Regular toxin analyses of shellfish samples indicated that domoic acid had been sporadically determined at shellfish breeding areas along the Eastern Adriatic

Coast (Ujević *et al*., 2010; Ljubešić *et al*., 2011; Arapov *et al*., 2016; Arapov *et al*., 2017). Reported concentrations of DA were always far below regulatory limits, as well as are reported values from other Adriatic regions (EU, 2004; Ciminiello *et al*., 2005; Ujević *et al*., 2010; Ljubešić *et al*., 2011; Pistocchi *et al*., 2012; Penna *et al*., 2013; Arapov *et al*., 2016; Arapov *et al*., 2017).

Despite significant interest in this genus, determination to species level remains challenging. The existence of cryptic and pseudo-cryptic species within this genus makes their identification, based solely on morphological characteristics, inadequate. Therefore, identification of *Pseudo-nitzschia* species, especially those belonging to the *P. pseudodelicatissima* and *P. delicatissima* groups, requires an integrated approach of morphological studies using light and electron microscopy with molecular phylogenetic analysis. Detailed taxonomic studies of *Pseudo-nitzschia* species can contribute to a better understanding of genus diversity and toxicity issues.

The aim of this study was to characterise *Pseudo-nitzschia* species composition during a high abundance period and to describe environmental conditions that enable *Pseudo-nitzschia* blooms in the Krka River estuary.

Material and Methods

Study area and sampling

The Krka River estuary is one of the major aquaculture areas along the Eastern Adriatic coast that, since 2000, is included in the National Monitoring Programme of regular shellfish and seawater quality controls. It is a highly stratified, 25 km long estuary, located in the central part of the Eastern Adriatic coast. A sharp halocline exists throughout the whole year in layers of 1m to 4m depth. Previous studies have confirmed that the halocline plays an important role in biogeochemical processes (Svensen *et al*., 2007) and represents an accumulation layer for freshwater and marine phytoplankton species (Viličić *et al*., 1989). Sampling was conducted in the middle estuary, at station Strmica (43.776320°N, 15.848007°E, depth 28 m, Fig. 1), over a two-month period, on the following sampling dates: 30th August, 13th September, 27th September, 2nd October, 10th October, 16th October and 25th October 2017.

Environmental parameters and shellfish toxin analyses

During the sampling period, seawater temperature and salinity were measured using a YSI Pro 1030 probe at four depths (surface, halocline, 5 m, 7 m). Concurrently with temperature and salinity measurements, phytoplankton and nutrient samples were collected using Nansen bottles at the same depths, except for 5 m (surface, halocline and 7 m depth).

Water samples for nutrient analyses were stored in the freezer immediately after sampling and transferred to the laboratory for further analyses. Concentrations of nitrates (NO_3^-), nitrites (NO_2^-), ammonium(NH_4^+), total nitrogen (Ntot), orthophosphates (PO_4^{3-}), total phosphates (Ptot) and orthosilicates (SiO_4^{4-}) were determined by a Seal Analytical Autoanalyzer III, according to the modified method used for nutrient determination in seawater (Grasshoff *et al*., 1999). Total inorganic nitrogen (TIN) was calculated as a sum of nitrates (NO_3^-), nitrites (NO_2^-) and ammonium(NH_4^+). Organic nitrogen (Norg) was calculated as a difference between concentrations of total nitrogen (Ntot) and total inorganic nitrogen (TIN), whereas organic phosphates (Porg) were calculated as a difference between total phosphates (Ptot) and orthophosphates (PO_4^{3-}) concentrations.

For the toxin analyses, samples of the mussel *Mytilus galloprovincialis* were collected concurrently with sampling of all other previously mentioned parameters throughout the investigated period. Domoic acid (DA) and epi-DA in shellfish samples were analysed by HPLC-DAD-UV system (Varian ProSTAR) according to Quilliam *et al*. (1995). Approximately 100 g of soft shellfish tissue was homogenised, and then a subsample of 8 g was prepared following the protocol proposed by Quilliam *et al*. (1995), including strong anion exchange (SAX) to avoid interference with tryptophan. A volume of 20 µL of sample was injected into the HPLC-DAD-UV system. The retention time of DA was close to 13 min. The limit

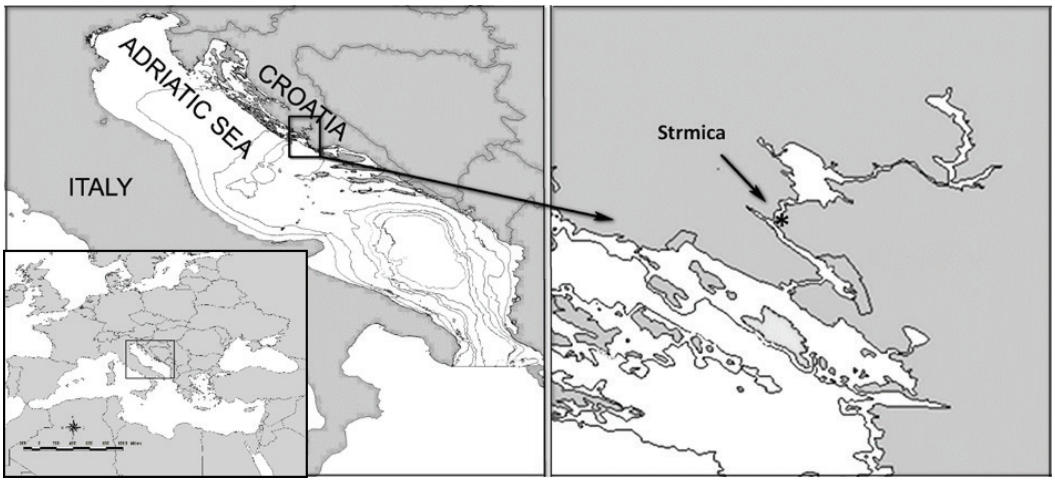

Fig. 1: Study area; the arrow indicates the Strmica sampling station, located in the Krka river estuary.

of detection (LOD) was 0.1025 µg DA g^{-1} and the limit of quantification was determined as 3 x LOD and was found to be 0.3415 µg DA g^{-1}. A detailed description of the HPLC method and composition of the mobile phase has been specified by Ujević *et al*. (2010) and Arapov *et al*. (2016).

Phytoplankton analyses (LM and SEM)

Phytoplankton composition and abundance were analysed using a Leica DMI4000B inverted light microscope(LM), according to the Utermöhl method (Utermöhl, 1958). After collection, the seawater samples (250 mL) were preserved with Lugol's solution and stored in the dark until the analyses. Subsamples of 25 mL were settled in counting chambers for at least 24 h, and then the cells were counted in one transect at 400x magnification and in half of the chamber bottom at 200x magnification.

The composition of *Pseudo-nitzschia* species was analysed using Field Emission Scanning Electron Microscopy (SEM, Tescan MIRA3), at the depth with the highest *Pseudo-nitzschia* spp. abundance determined by LM. Organic material from the valves was removed by adding 10% hydrochloric acid (HCl), 30% sulphuric acid (H_2SO_4), concentrated potassium permanganate ($KMnO_4$) and, after 24 h, concentrated oxalic acid $(COOH)_2$. Subsequently, the sample was rinsed three times in distilled water, as described by Arapov *et al*. (2017). In each sample, the first 50 valves were measured: the length, width, number of fibulae and interstriae in 10 µm, as well as the number of poroids in 1 µm and number of sectors observed within poroid. The observed morphological characteristics were compared to the data available in the literature in order to determine *Pseudo-nitzschia* species.

Samples for morphological analyses of established *Pseudo-nitzschia* cultures were prepared according to Hasle & Fryxell (1970) in order to observe the characteristics of the girdle band. Subsamples of 500 µL of the cleaned samples were filtered through polycarbonate membrane filters (pore size 1 µm, Nucleopore, Whatman), dried for at least 24 h in a desiccator, coated with gold and examined with SEM. The first twenty intact valves of each cultured strain were measured.

Cell isolation and molecular analyses

Pseudo-nitzschia strains were isolated from field seawater samples collected with a plankton net (20 µm pore size), towed from 7 m to the surface. Single-cells or a chain was isolated under a Leica DMI4000B inverted light microscope using a sterile glass micropipette. Isolated cells were transferred to a 24-well tissue culturing plate, containing 1 mL of f/2 medium and kept at 21°C, with a 12:12 (light:dark) photoperiod at 108 µmol photons m^{-2} s^{-1}. Upon the observed growth, isolates were transferred to culturing flasks containing 30 mL of f/2 medium and were further analysed. Isolated strains were fixed with Lugol's solution on the seventh day of transfer of the strains to a culturing flask for detailed morphological analyses by SEM, as described above.

Moreover, two cultured strains of *Pseudo-nitzschia* spp. were analysed for species-specific taxonomical assignment by LSU and ITS- 5.8S rDNA sequence alignment. The sequences of ribosomal genes obtained from two *Pseudo-nitzschia* cultured isolates were deposited in the NCBI GenBank. The accession number of P2B5 and P2E5 strains are MN545365 and MN545366 for the LSU gene, respectively and MN545442 and MN545443 for the ITS-5.8S gene, respectively. For genomic DNA extraction, the exponential phase cultures of *Pseudo-nitzschia* spp. were harvested by centrifugation at 4,000xg for 20 min at room temperature. Total genomic DNA was extracted from cell pellets using a DNeasy Plant Kit (Qiagen, Valencia, CA, USA), according to the manufacturer's instructions. Quantification was performed using a Qubit fluorometer with a Quant-iT dsDNA HS Assay Kit (Invitrogen, Carlsbard, CA, USA). Then, the LSU rDNA was amplified and sequenced using D1R and D2C primers (Scholin *et al*., 1994) targeting the D1-D2 region. The ITS-5.8S region of the rDNA was amplified and sequenced using the universal primers ITSA and ITSB (Adachi *et al*., 1994). The PCR reaction for LSU rDNA and ITS-5.8S rDNA was as follows: tubes contained 25 µl of 1X reaction buffer (Hot Start Taq DNA Polymerase 5U/µl, Biotechrabbit GmbH, Germany), 2.5 mM of $MgCl_2$, 0.75X PCR Enhancer, 200 µM of dNTPs, 200 nM or 400 nM of each primer for ITS and LSU, respectively, 1U Taq DNA Polymerase and 0.5-1 ng of DNA template. PCR thermal cycling conditions were the same as reported in Pugliese *et al*. (2017). All amplified PCR products were purified using a MinElute Gel Extraction Kit (Qiagen), and the products were directly sequenced with the ABI PRISM BigDye Terminator Cycle Sequencing Kit v. 1.1 on an ABI 310 Genetic Analyzer (Applied Biosystem, Foster City, CA, USA). Standard thermal cycling conditions were used for both templates, setting the annealing temperature according to the template (60° C and 50° C for ITS and LSU PCR specific primers, respectively). Difficult templates and repeated regions were solved by increasing initial denaturation time and modifying the thermal cycling condition as follows: 40 cycles of denaturation at 96° C for 10 s and annealing/extension at 50° C for 4 min.

Phylogenetic analyses

Analyses on the D1-D2 region of LSU rDNA and ITS-5.8S were conducted separately. The LSU and ITS-5.8S sequences were aligned using MAFFT software. Short aligned sequences and ambiguously aligned positions were excluded from the alignment, manually or using Gblocks (http://molevol.cmima. csic.es/castresana/Gblocks.html) with default settings. The neighbor-joining (NJ), maximum parsimony (MP) and maximum likelihood (ML) analyses were performed in MEGA v. 7.0. The robustness of the NJ, MP and ML trees was tested by bootstrapping using 1000 pseudo-replicates. Distance and

maximum likelihood trees were built based on the substitution model selected through the Akaike Information Criterion option implemented in MEGA v. 7.0 (Kumar *et al.,* 2016). The most appropriate evolutionary models for LSU and ITS-5.8S gene rDNA alignment were found to be HKY + G + I and Tamura-Nei + G, respectively, with gamma distribution values of 0.59 and 0.35, respectively. The MP analyses were performed using the Tree-Bisection-Redrafting (TBR) algorithm with search level 1, in which the initial trees were obtained by the random addition of sequences (10 replicates). All positions containing gaps and missing data were eliminated. Bayesian analyses were performed using MrBayes ver. 3.2.6 (Ronquist & Huelsenbeck, 2003) as implemented in Genious Prime 2019.2 (Kearse *et al*., 2012) using the GTR + G model for all analyses. Four independent Markov Chain Monte Carlo simulations were run simultaneously for 2,000,000 generations. Trees were sampled every 100 generations, and 2,001 trees were discarded as burn-in. The sequences of *Fragilariopsis rhombica* 5–17 AF7656 and *Fragilariopsis* sp. NL2010 GU170665 were used as an outgroup for the *Pseudo-nitzschia* LSU and ITS-5.8S gene phylogenetic analyses, respectively.

Statistical analyses

Vertical distribution of temperature and salinity were presented using Ocean Data View software-ODV (Schlitzer, 2018), while nutrient concentrations were presented with graphs created using the Statistica 13.0 software package. The Pairwise Spearman rank correlations were performed using the Statistica 13.0 software package on non-transformed data of *Pseudo-nitzschia* spp. abundance and environmental data and between salinity and nutrient concentrations. In order to explore the relationship between *Pseudo-nitzschia* abundance and environmental parameters Principal Component Analysis (PCA) was performed on a transformed (log(x+1) for *Pseudo-nitzschia* abundance) and normalized dataset, using the PRIMER 6 (Clarke & Warwick, 2001) software package.

Results

Description of environmental parameters

The highest seawater temperature (24° C) was recorded in the surface layer at the beginning of sampling (30th August). On the following sampling date (13th September), seawater temperature was uniform at all sampling depths, while afterwards a cooling of the surface layer was noticed. Salinity in the upper two sampling layers was very variable, and an halocline was continuously present in the layer between 1 m to 3 m depth. The most pronounced halocline was recorded at the end of September, when the lowest value of surface salinity was measured (14.3). Salinity values at 7 m depth were rather constant, ranging from 37.7 to 38.7 (Fig. 2).

The pre-bloom period was characterised by the highest concentration of ammonium (6.51 µM), orthophosphates (0.26 µM) and organic phosphates (0.69 µM). The elevated concentrations and maximum values of other inorganic nitrogen forms were: NO_3^-=9.61 µM; NO_2^-=0.24 µM, organic nitrogen 15.80 µM, and orthosilicates 31.96 µM. These values were determined at the end of September and thereafter, coinciding with a period of decreased surface salinity due to higher river discharge (https://hidro.dhz.hr/) (Fig. 3).

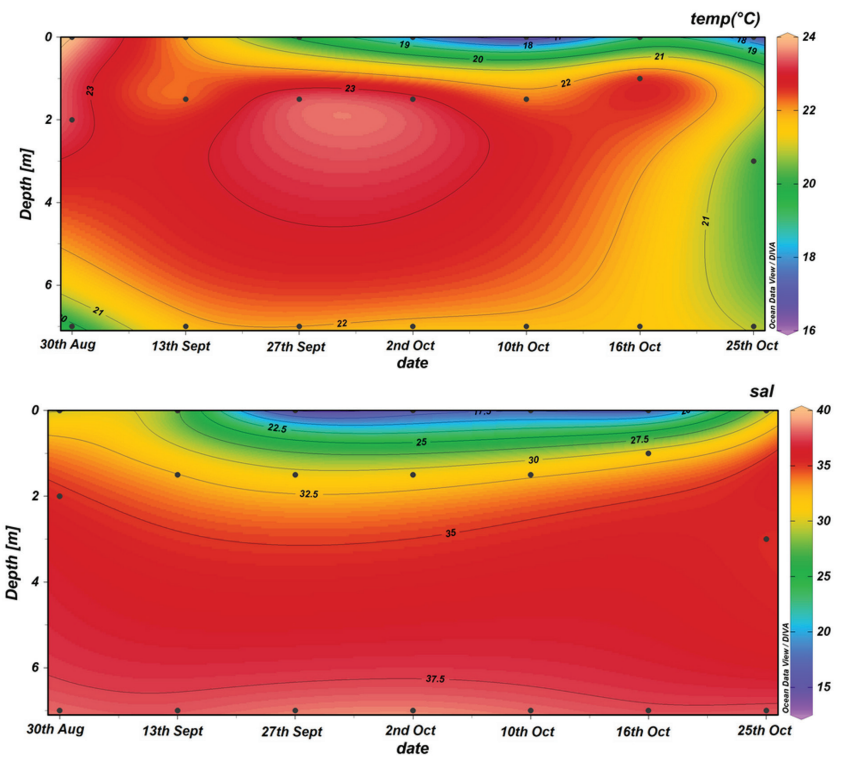

Fig. 2: Vertical profile of temperature and salinity at Strmica sampling station during the investigated period.

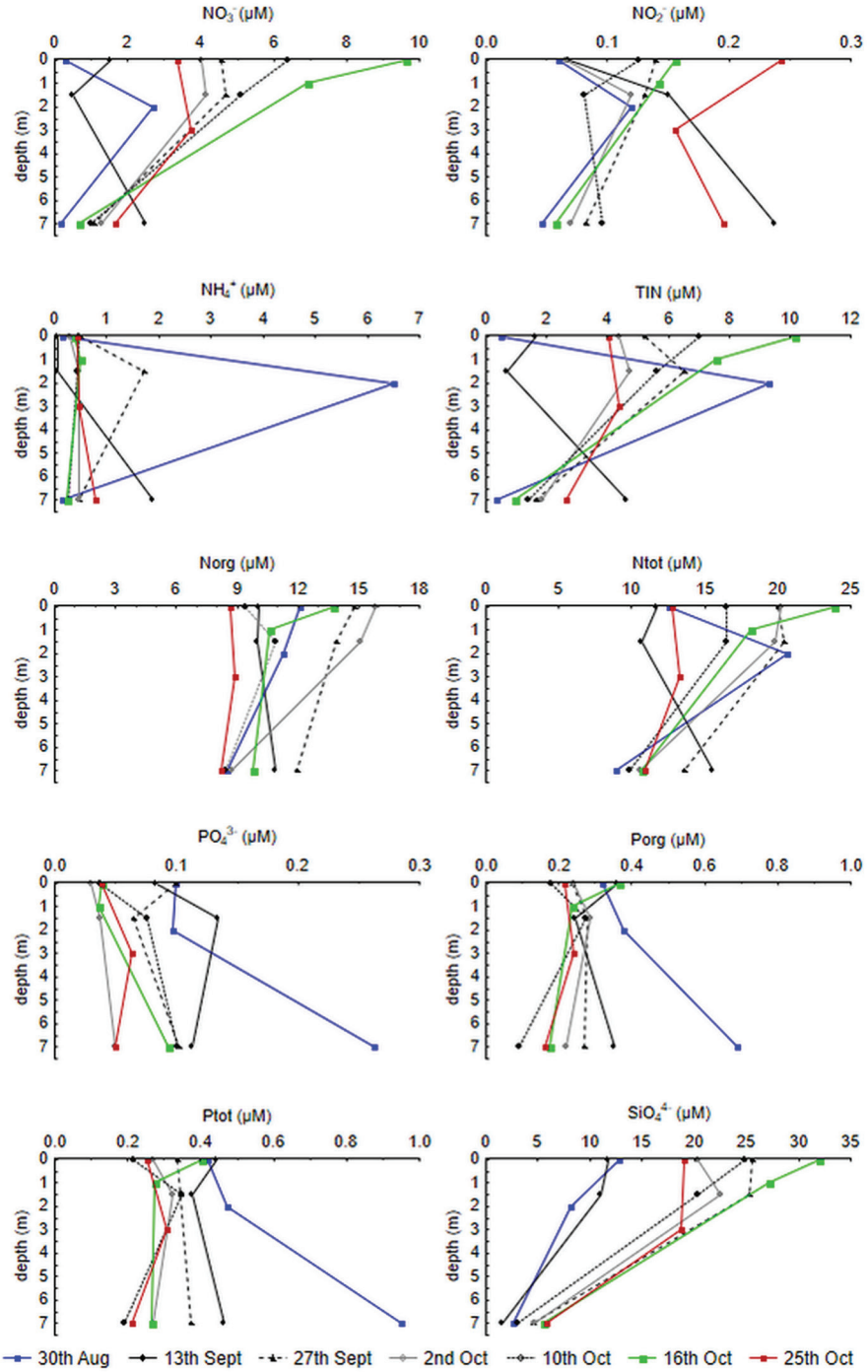

Fig. 3: Vertical distribution of nutrient concentrations (nitrates (NO_3^-), nitrites (NO_2^-), ammonium (NH_4^+), inorganic nitrogen (TIN), organic nitrogen (Norg), total nitrogen (Ntot), orthophosphates (PO_4^{3-}), organic phosphates (Porg), total phosphates (Ptot) and orthosilicates (SiO_4^{4-})) at Strmica sampling station during the investigated period.

Pseudo-nitzschia* spp. *assemblage composition and toxin analyses

Light microscopy analyses demonstrated that diatoms were dominant at the sampling depth of 7 m, representing 77.8-96.3% of the phytoplankton community throughout the investigated period. In the upper two sampling layers (surface and halocline), intense coccolithophore blooms were recorded in August and October, representing 72.6 and 90.6% of the phytoplankton assemblage, respectively (data not shown).

The highest abundance of *Pseudo-nitzschia* spp. was recorded on the 13th of September at 7m depth, reaching 1.8 x 10^6 cells L^{-1}, at a temperature of 21.8°C and and a salinity of 37.9. Within the following four weeks, abundance decreased, but it was still high, in the range of 3.0 x 10^5 to 7.2 x 10^5 cells L^{-1}. At the end of October, abundance notably dropped to 2.8 x 10^3 cells L^{-1}, and was recognised as the end of blooming. Comparing the sampling layers, the highest abundance of *Pseudo-nitzschia* was recorded at 7 m depth, except at the end of August when slightly higher values were recorded at the surface and halocline,

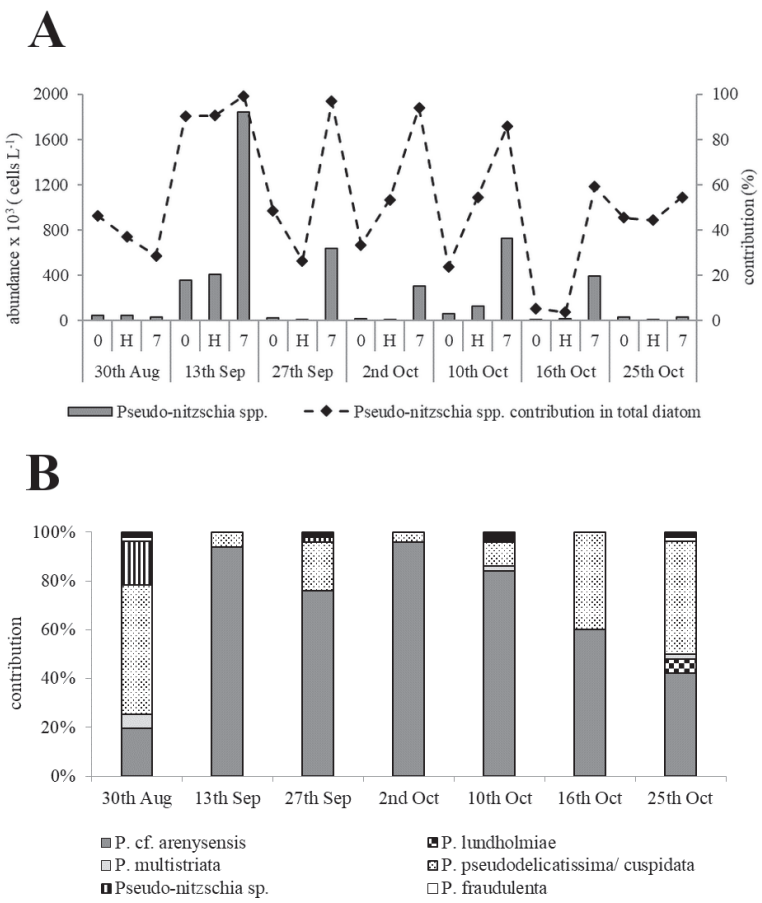

Fig. 4: A) Abundance of *Pseudo-nitzschia* spp. (cells L^{-1}) and its contribution to the diatom community (%), determined by Light Microscopy analyses; B) composition of *Pseudo-nitzschia* species at 7 m sampling depth obtained by Scanning Electron Microscopy.

which was at 2 m. The contribution of *Pseudo-nitzschia* spp. to the diatom community showed a similar pattern to that of abundance. The maximum percentage, above 90%, was recorded on the 13th of September at all sampling depths, and remained high during the following three weeks, representing over 85% in 7 m deep layer (Fig. 4A).

Toxin analyses of shellfish samples confirmed that concentrations of DA and epi-DA were always below LOD, throughout the entire investigated period.

Pseudo-nitzschia species composition and morphology

Morphological characterisation by Scanning Electron Microscopy analyses revealed that *P.* cf. *arenysensis* contributed to 94% of the *Pseudo-nitzschia* community at the peak of abundance. During the investigated period, *P.* cf. *arenysensis* mostly dominated over the other species, except in the pre-bloom period (30th Aug) and at the end of October when *P. pseudodelicatissima*/*cuspidata* prevailed. Besides the mentioned species, other taxa of *Pseudo-nitzschia* were identified in low contribution, including *P. lundholmiae*, *P. multistriata*, *P. fraudulenta*, *P. subfraudulenta* and *Pseudo-nitzschia* sp.-a morphotype similar to *P. pseudodelicatissima*/*cuspidata* (Fig. 4B). The species *P. lundholmiae* was documented for the first time in the Adriatic Sea, as well as *P. multistriata* along the Eastern Adriatic coast. The morphological characteristics of the species observed in the field samples are presented in Table 1.

Pseudo-nitzschia cf. *arenysensis*

In valve view, the cells are lanceolate and symmetric, gradually tapering towards the round apices. The eccentric raphe is divided by a central interspace with a central nodule. The central interspace occupies two to almost five striae. Fibulae are irregularly spaced. Each stria contains two rows of rounded poroids, located close to the interstriae (Fig. 5A).

Pseudo-nitzschia lundholmiae

The cells are lanceolate with rounded apices (Fig. 6 A, C). A central interspace with central nodule is present and occupies four to five striae. The fibulae are irregularly spaced. Usually twice more interstriae than fibulae were observed in 10 μm. Each stria comprises of one row of poroids or two rows of small poroids (Fig. 6B). In general, poroids at uniseriate striae were mostly divided into two sectors (69.7%) and rarely three (23.6%) or four

Table 1. Morphological features of the observed *Pseudo-nitzschia* species obtained by SEM. Number of measured cells are given in parentheses (n), minimum and maximum values are given in bold, while the average ± standard deviation are specified below.

Species (n)	Width (µm)	Length (µm)	CN	Fibulae (10µm)	Interstriae (10µm)	Poroid rows	Poroids (1µm)	Sectors in poroids
P. cf. *arenysensis* (246)	**0.99-1.77**	**44.39-76.87**	+	**20-26**	**37-42**	2	**9-12**	/
	1.28±0.12	52.35±3.97		22.4±1.12	38.5±0.75			
P. lundholmiae (7)	**1.62-2.04**	**52.56-68.76**	+	**16-18**	**33-35**	1-2	**5-6**	**2-4** (208)
	1.83±0.13	59.61±8.31		17±0.82	33.7±0.75			
P. multistriata (10)	**1.97-2.30**	**63.89-77.18**	-	**24-25**	**38-41**	1-3	**10-12**	/
	2.13±0.11	71.04±4.59		24.8±0.42	39.2±1.03			
P.pseudodelicatissima/ cuspidata (125)	**1.1-1.48**	**75.24-134.83**	+	**16-22**	**32-37**	1	**4-6**	**1-5** (1076)
	1.26±0.07	105.57±12.08		19.2±1.28	35.5±0.79			
P. fraudulenta (4)	**4.22-4.92**	**87.10-102.92**	+	**21-23**	**23-24**	2-3	**5-7**	several
	4.50±0.32	97.63±7.41		21.75±0.95	23.5±0.58			
P. subfraudulenta (13)	**3.16-3.93**	**100.66-139.40**	+	**14-16**	**23-26**	1-3	**5-6**	**2-7** (102)
	3.57±0.24	114.87±12.13		17.77±0.60	24.76±0.83			
Pseudo-nitzschia sp. (17)	**1.01-1.40**	**48.29-63.52**	+	**21-24**	**40-41**	1	**5-7**	**1-2** (78)
	1.17±0.09	56.12±3.84		22.82±0.73	40.35±0.49			

(6.3%). In biseriate striae sectors within poroids were not observed.

Pseudo-nitzschia pseudodelicatissima /cuspidata

In the valve view, the cells are linear and symmetric with short tapering ends. A central interspace with central nodule is present and corresponds to 3 to 6 striae. On the eccentric raphe, the fibulae are irregularly spaced. The striae compose one row of large rounded to squared poroids, divided mainly in two (56.7%) or three (26.6%) sectors. Poroids that were not divided into sectors (2.9%) or comprising four (13.0%) or five sectors (0.8%) were rare.

Pseudo-nitzschia multistriata

In the valve view, the cells are slightly asymmetric and linear in the middle part, sharply tapered toward the ends (Fig. 6 D). The central nodule is absent. The frustules are weekly silicified, with wide striae and narrow interstriae. Furthermore, irregular interstriae are noticed where some neighbouring interstriae merge into one, close to the raphe canal (Fig. 6 E). The striae are composed of mainly two (occasionally one or three) rows of small rounded poroids, placed close to the interstiae (Fig. 6 E). Opposite ends of the same valve differ in their ultrastructure (Fig. 6 F, G).

Pseudo-nitzschia fraudulenta

The cells are symmetric and lanceolate, in valve view. A central interspace with central nodule is present. The central interspace occupies three to five striae. The number of fibulae corresponds to the observed number of striae. Each stria usually has two rows of poroids, but occasionally one or three rows were also noticed. The poroids are usually divided into several irregular sectors.

Pseudo-nitzschia subfraudulenta

In the valve view, the cells are symmetric and linear in the middle part, with pointed ends. A central nodule is present, and the central interspace occupies three to five striae. Each stria usually consists of two rows of poroids, rarely one or three rows. The poroids are mainly divided into three to five sectors (83.4%) but poroids with two (6.9%), six (8.8%) or seven (1.0%) sectors were observed, albeit rarely.

Pseudo-nitzschia **sp.**

The cells are symmetric, linear to lanceolate, gradually tapering toward pointed apices (Fig. 6 H, J). A central nodule is present and the central interspace occupies three to five striae, while the fibulae are irregularly spaced (Fig. 6 I, J). Each stria contains one row of big squared poroids, which are mostly undivided into sectors or, occasionally, two sectors were noticed (Fig. 6 I).

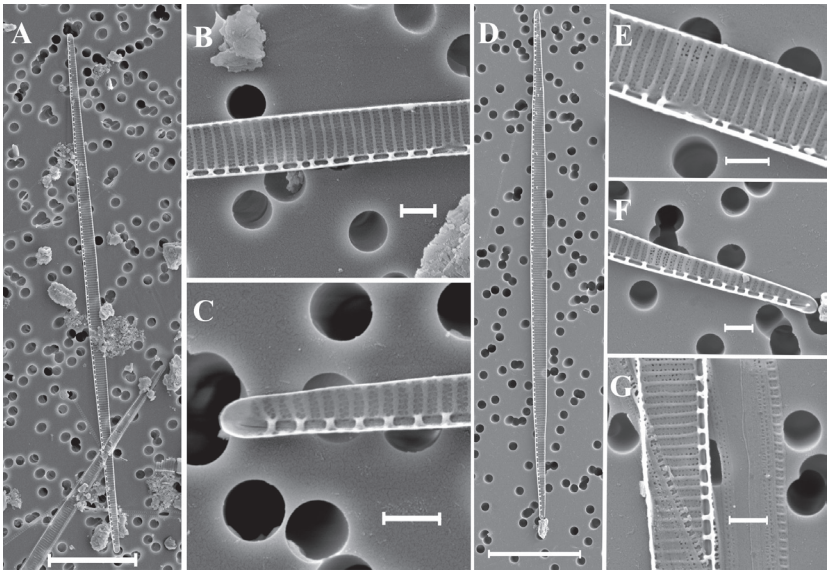

Fig. 5: A-C) *Pseudo-nitzschia* cf. *arenysensis* in field samples obtained by SEM: A) whole valve; B) central part of the valve showing central interspace and structure of the striae; C) valve end. D-G) *Pseudo-nitzschia* cf. *arenysensis* (P2E5) in culture: D) whole valve; E) central part of the valve showing central interspace with central nodule; F) end of the valve; G) structure of cingulum. Scale bars represent: A, D =10 µm; B, C, E, F, G =1µm.

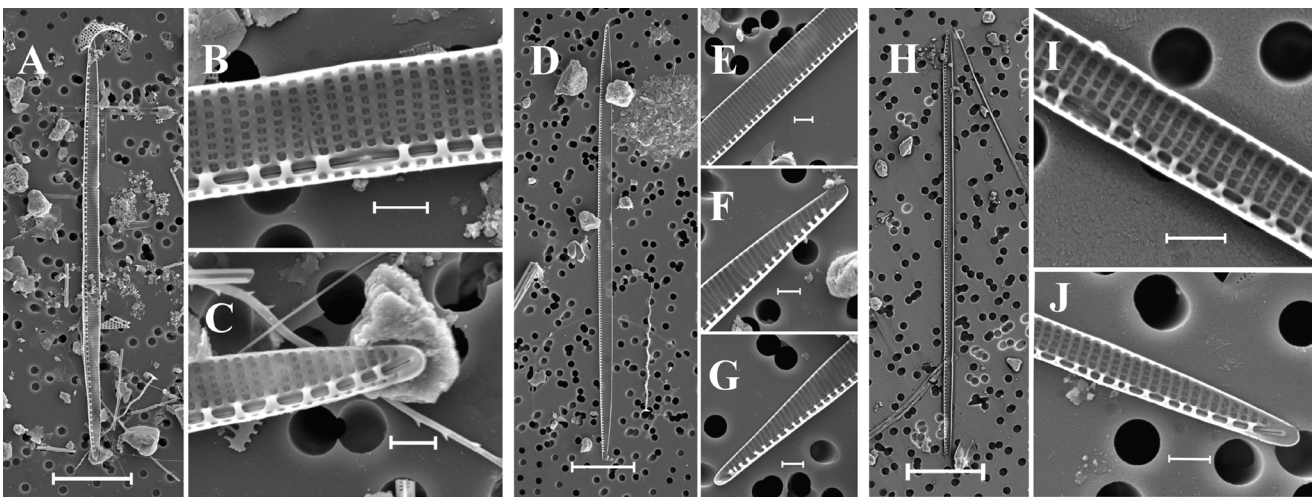

Fig. 6: A-C) *Pseudo-nitzschia lundholmiae* in SEM: A) whole valve; B) central part of the valve showing central interspace and structure of the striae; C) valve end. D-G) *Pseudo-nitzschia multistriata* in SEM: D) whole valve; E) central part of the valve showing the irregular structure of the striae; F-G) opposite ends of the same valve. H-J) *Pseudo-nitzschia* sp. observed by SEM: H) whole valve; I) central part of the valve showing central interspace with central nodule; J) end of the valve. Scale bars represent: A, D, H =10 µm; B, C, E, F, G, I, J =1µm.

Morphological description of the cultured strains of P. cf. *arenysensis*

The valves of both isolated strains (P2B5 and P2E5) are lightly silicified and lanceolate with slightly rounded and blunt ends (Fig. 5 D). Morphologically, the valves of cultured strains showed minor differences in the measured valve length, minimum number of fibulae, maximum number of interstriae (Table 2). The cingulum is composed of three bands. The first band, valvolcopula, consists of one row of large rectangular poroids, divided mostly into 3-4 sectors, in general, two poroids wide and two high (2x2). The second band is perforated, and the third unperforated (Fig. 5 G). The morphological characteristics of the *P.* cf. *arenysensis* isolated strains observed by SEM are presented in Table 2, including data of other morphologically similar *Pseudo-nitzschia* species obtained from the literature.

Phylogenetic analyses of Pseudo-nitzschia spp. *LSU and ITS-5.8 S ribosomal genes*

The final alignment of *Pseudo-nitzschia* spp. ribosomal gene sequences, such as LSU and ITS-5.8S, with *Fragilariopsis* as an outgroup, were as follows: LSU was 794 bp in length (A = 21.2%, T = 29.7%, C = 18.2%, G = 30.6%) with 777 total informative sites, excluding gaps, and 552 polymorphic sites, of which 529 were parsimony sites. ITS-5.8S was 1020 in length (A = 23.08%,

Table 2. Comparison of morphological characteristics of two cultured strains of *P.* cf. *arenysensis* (P2B5, P2E5) and other similar *Pseudo-nitzschia* species reported in literature. Number of measured cells are given in parentheses (n), minimum and maximum values are given in bold, while the average ± standard deviation are specified below.

Species (n)	Width (µm)	Length (µm)	CN	Fibulae (10µm)	Interstriae (10µm)	Poroid rows	Poroids (1µm)	Band striae (10µm)	References
P. cf. *arenysensis* P2B5 (20)	**1.51-1.84**	**46.51-54.54**	3-4.5	**20-23**	**37-41**	2	**9-11**	**44-46**	This study
	1.66±0.10	51.53±2.55	3.79±0.38	21.75±0.97	38.15±0.93		10.30±0.57	44.8±0.7	
P. cf. *arenysensis* P2E5 (20)	**1.54-1.97**	**54.05-56.33**	3-6	**18-23**	**37-39**	2	**9-11**	**43-45**	This study
	1.73±0.10	55.74±0.59	4.13±0.78	20.65±1.04	37.95±0.60		10.23±0.53	44.4±0.6	
P. arenysensis	1.6-2.7	22-59	Yes	17-26	32-45	2	7-12	40-50	Quijano-Scheggia *et al*., 2009; Quijano-Scheggia *et al*., 2010; Ajani *et al*., 2013; Orive *et al*., 2013
P.delicatissima/P. arenysensis	1.2-2.2	32-70	Yes	20-27	32-41	2	8-12	48-49	Teng *et al*., 2013; Stonik *et al*., 2011
P. delicatissima	0.8-2.6	19-76	Yes	18-28	32-45	2	7-14	40-50	Lundholm *et al*., 2006; Quijano-Scheggia *et al*., 2008a; Moschandreou & Nikolaidis, 2010; Marić Pfannkuchen, 2013; Orive *et al*., 2013; Stonik *et al*. 2018; Turk Dermastia *et al*., 2020
P. decipiens	1.1-2.4	27-64	Yes	20-26	41-46	2	9-13	/	Lundholm *et al*., 2006; Teng *et al*., 2013
P. dolorosa	1.6-3.0	29.9-72	Yes	18-22	30-38	1-2	5-8	40-47	Lundholm *et al*., 2006; Marchetti *et al*., 2008; Rivera-Vilarelle *et al*., 2013; Teng *et al*., 2013
P. hallegraeffii	1.9-3.1	25.6-55.4	Yes	16-22	34-40	2(1)	6-8	43-56	Ajani *et al*., 2018

T = 30.3%, C = 22.9%, G = 23.71%) with 521 total informative sites excluding gaps and 244 polymorphic sites, of which 198 were parsimony sites. Based on single LSU and ITS-5.8S rDNA sequences, only minor differences among NJ, MP, ML and Bayesian inference analyses were found; therefore, only ML phylogenetic trees are presented. The LSU rDNA phylogeny that was obtained from 43 isolates of *Pseudo-nitzschia* spp. showed that Croatian strains, P2B5 and P2E5, grouped with isolates of *P. arenysensis*, a sister clade of *P. delicatissima/micropora/dolorosa.* The clade was supported by high bootstrap and posterior probability values (Fig. 7 A). The ITS-5.8S rDNA phylogeny obtained from 34 isolates of *Pseudo-nitzschia* spp. showed similar topology to the LSU rDNA phylogeny, confirming that the Croatian strains identified as *P.* cf. *arenysensis* by microscopy analysis grouped into the clade of *P. arenysensis*, which segregated after *P. delicatissima*. These two clades diverged after *P. micropora.* All the clades were supported by high bootstrap and posterior probability values (Fig. 7 B).

Statistical analyses

Single Spearman rank correlations showed that *Pseudo-nitzschia* spp. abundance significantly correlated with salinity and inorganic nutrients. A positive correlation was recorded with salinity and orthophosphates and a

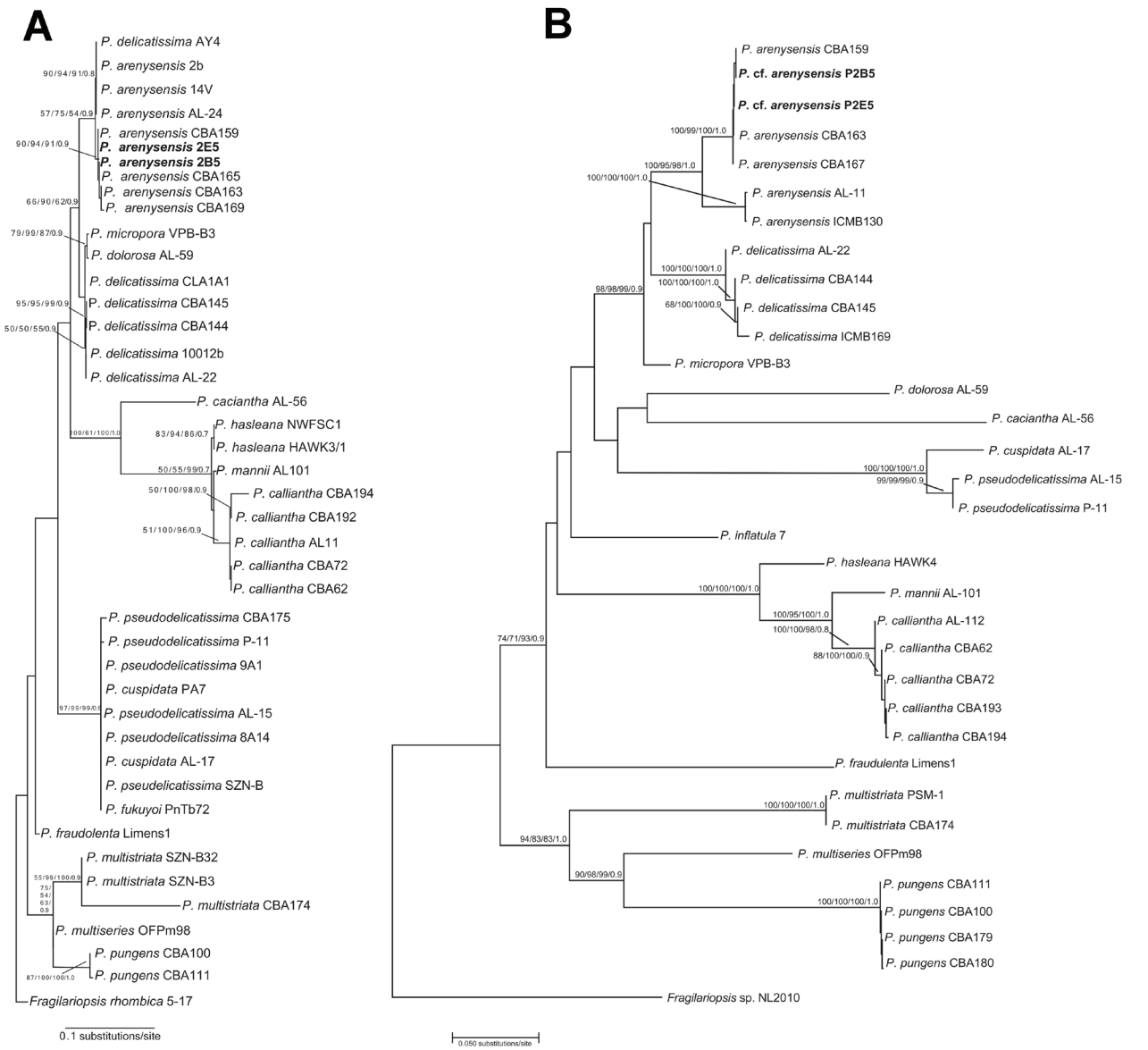

Fig. 7: A) Maximum likelihood phylogenetic tree of the genus *Pseudo-nitzschia* inferred from LSU rDNA. The tree was rooted with *Fragilariopsis rhombica* 5-17 as outgroup. Numbers of the major nodes represented from left to right NJ, (1000 pseudoreplicates), MP (1000 pseudoreplicates), ML (1000 pseudoreplicates), bootstrap and Bayesian posterior probability values. Only bootstrap values > 50% were shown. B) Maximum likelihood phylogenetic tree of the genus *Pseudo-nitzschia* inferred from ITS -5.8S rDNA. The tree was rooted with *Fragilariopsis* sp. NL2010 as outgroup. Numbers of the major nodes represented from left to right NJ, (1000 pseudoreplicates), MP (1000 pseudoreplicates), ML (1000 pseudoreplicates), bootstrap and Bayesian posterior probability values. Only bootstrap values > 50% were shown. Sequences of bold isolates were obtained in this study.

negative correlation with nitrates and orthosilicates (Table 3).

Principal Component Analysis (PCA) showed that the first two principal components PC1 (40.3%) and PC2 (17.7%) explain 58.0% of total variance within the dataset (Fig. 8). The first one (PC1) showed a positive association with orthosilicates (0.481), nitrates (0.462) and a negative one with salinity (-0.448). The second principal component (PC2) showed the strongest association with organic phosphorus (-0.602).

In the investigated area, the Krka River is the main source of nitrogen and silicates (Cetinić *et al*., 2006). Therefore, to determine the origin of nutrients, the Spearman rank correlation was performed between salinity and nutrient concentrations. A statistically significant negative correlation was confirmed for salinity with nitrates, TIN, Norg and orthosilicates and a positive correlation with orthophosphates (Table 3).

Discussion

Morphology of Pseudo-nitzschia spp.

In this study, the *Pseudo-nitzschia* assemblage was morphologically characterised before and during the blooming period in the Krka River estuary. Scanning Electron Microscopy and phylogenetic analyses confirmed *P.* cf. *arenysensis* as the dominant species in the *Pseudo-nitzschia* community during this bloom event. Although *Pseudo-nitzschia* species are abundant and often represent the majority of a diatom community along the eastern Adriatic coast, species composition during high proliferation events include only bloom report (>10^6 cells L^{-1}) for *P. calliantha* (Burić *et al*., 2008; Ljubešić *et al*., 2011; Marić *et al*., 2011). In the majority of the previous studies, due to the limitation of the commonly used light microscopy technique (LM), bloom events were reported as a complex of *Pseudo-nitzschia* species (Viličić *et al*., 2009; Ujević *et al*., 2010; Bužančić *et al*., 2012; Marić *et al*., 2012).

Throughout the investigated period, seven *Pseu-*

Table 3. Spearman rank correlation coefficients between salinity and *Pseudo-nitzschia* spp. abundance with physical and chemical parameters. Statistically significant correlations ($p<0.05$) are presented in bold; *$p<0.01$; **$p<0.001$.

	T	S	NO_3^-	NO_2^-	NH_4^+	TIN	Norg	PO_4^{3-}	Porg	SiO_4^{4-}
Salinity	/	/	**-0.59***	-0.14	0.1	**-0.46**	**-0.55***	**0.48**	-0.09	**-0.82****
Pseudo-nitzschia spp.	0.12	**0.52**	**-0.59***	-0.24	-0.27	**-0.49**	-0.35	**0.61***	-0.14	**-0.72****

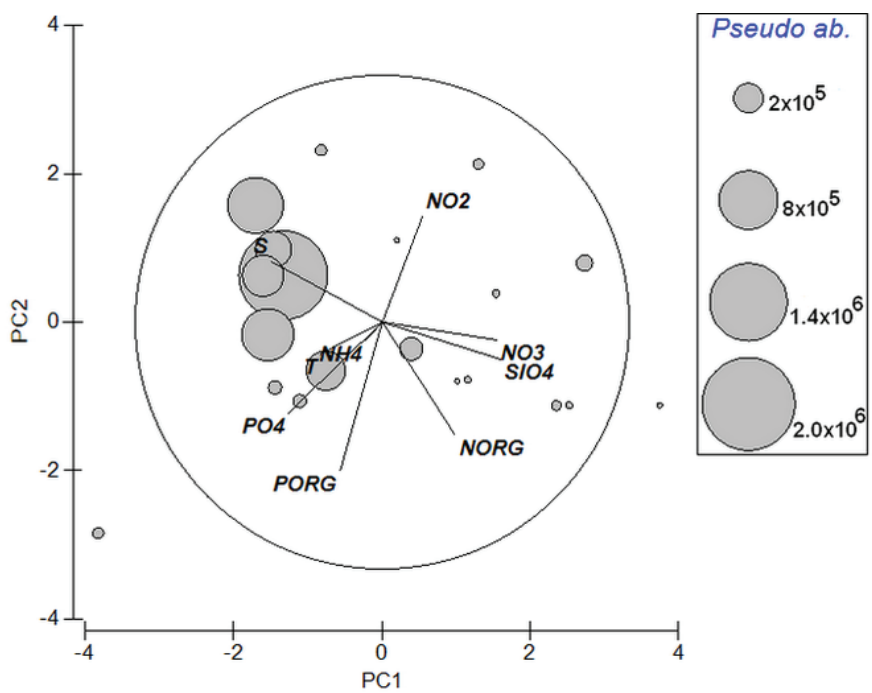

Fig. 8: Scatterplot of the first two principal components, following PCA of environmental parameters and the abundance of *Pseudo-nitzschia* spp. (cells L^{-1}).

do-nitzschia species were morphologically determined. Besides the previously reported *P. pseudodelicatissima* and *P. subfraudulenta* (Arapov *et al*., 2016), species *P.* cf. *arenysensis*, *P. multistriata*, *P. lundholmiae* and *P. fraudulenta* are newly described from Krka river estuary. The finding of *P*. *multistriata* is a new record for Central Adriatic waters, while *P. lundholmiae* morphologically corresponds to *Pseudo-nitzschia* sp. formerly described from Kaštela Bay (Arapov *et al*., 2017).

The dominant species *P*. cf. *arenysensis*, based on its morphological features, belong to the *P. delicatissima* species complex. Morphologically, the only difference between *P. arenysensis* and *P. delicatissima* is the range of the valve width. According to the data available in the literature (Table 2), the thicker specimens are reported for *P. arenysensis*, while the width range of *P. delicatissima* is much wider, including the minimum value (0.8 µm) documented from the Adriatic Sea (Marić Pfannkuchen, 2013). Considering that in this study the maximum measured valve width was greater than previously reported from the Central Adriatic Sea (Arapov *et al*., 2017), this species was characterised as *P*. cf. *arenysensis*. Phylogenetic analysis based on the ITS and LSU rDNA sequences confirmed that the Croatian strains grouped with *P. arenysensis*.

Specimens of *P.* cf. *arenysensis* from the field samples and cultures displayed similar morphological characteristics. Slightly larger valve width and a lower number of fibulae were observed in cultures (18 fibulae for cultured strain P2E5; Table 1, Table 2). In general, the number of fibulae for *P. arenysensis* ranges from 20 to 28 (as specified in Table 2), but a minimum of 17 fibulae has been reported by Orive *et al*. (2013). The number of bend striae in our cultured strains (43-46) perfectly fits the reported range for *P. arenysensis* from the Western Mediterranean: 40-50 (Quijano-Scheggia *et al*., 2009; Quijano-Scheggia *et al*., 2010) and south-east Australia: 40-46 (Ajani *et al*., 2013). The observed differences in morphology of cultured *Pseudo-nitzschia* cells and those observed in field samples could be due to the growing conditions. The morphology of diatom frustules can be affected and controlled by environmental conditions, such as temperature, salinity, light, pH, light, heavy metals, biotic factors, etc. (Su *et al*., 2018). In *Pseudo-nitzschia seriata*, an increase in temperature caused a decrease in the number of rows of poroids within striae and the density of poroids. However, no changes were observed in the density of interstriae and fibulae per 10 µm and in valve width (Hansen *et al*. 2011). Authors Montages & Franklin (2001) showed that cell size (volume) decreased with increasing temperature, while Marchetti & Harrison (2001) demonstrated that the valve transapical axis decreased in several *Pseudo-nitzschia* under iron-deficiency conditions.

The morphological features of *P. pseudodelicatissima/cuspidata*, *P. subfraudulenta*, *P. fraudulenta*, are consistent with those previously reported from the Adriatic Sea and worldwide (Ljubešić *et al*., 2011; Moschandreou *et al*., 2012; Marić Phannkuchen, 2013; Teng *et al*., 2013; Arapov *et al*., 2016; Arapov *et al*., 2017; Turk Dermastia *et al.*, 2020).

A comparison of the morphometry of *P. multistriata* from Krka river estuary with the data available in the literature, showed that the specimens found differ as to the length of the transapical axis. In our study, the measurements of valve width ranged between 1.97 and 2.30 µm, which corresponds to the range reported by Teng *et al*. (2013) but is narrower in comparison to 2.2-4.6 µm range reported by the majority of other authors (Orsini *et al*., 2002; Orlova *et al*., 2008; Quijano-Scheggia *et al*., 2008a; Moschandreou & Nikolaidis, 2010; Sahraoui *et al*., 2011; Stonik *et al*., 2011; Ajani *et al*., 2013; Rivera-Vilarelle *et al*., 2013; Stonik *et al*., 2018; Turk Dermastia *et al.*, 2020).

The morphology of *Pseudo-nitzschia lundholmiae* corresponds to the original description (Lim *et al*., 2013), including valve shape, length, width and number of fibulae and interstriae measured (10 µm). The main difference concerns the number of sectors within poroids. In specimens from our study, four sectors were observed in a low percentage of poroids (6.3%) as opposed to the three sectors at the most reported by Lim *et al*. (2013) and Teng *et al*. (2016).

In addition, undetermined *Pseudo-nitzschia* sp. morphologically resemble *P. pseudodelicatissima/cuspidata*, a species that commonly occurrs in the waters of the central Adriatic. As it fits within the reported ranges of morphometric values for *P. pseudodelicatissima/cuspidata,* it could easily be included in this species complex. The main differences observed that distinguish *Pseudo-nitzschia* sp. from *P. pseudodelicatissima/cuspidata* were: shape of poroids that are mostly squared without sectors; larger number of interstriae, 40-41 in comparison to 32-37 observed for *P. pseudodelicatissima/cuspidata*; shorter transapical axis (Table 1, Fig 6 H-J). Apart from morphological characterisation, one of our future research focuses will be a confirmation of these species, combining morphology with molecular methods.

The majority of *Pseudo-nitzschia* species found are confirmed as potentially toxic, but the dominant *P.* cf. *arenysensis* is considered as non-toxic (Lundholm, 2019). Accordingly, toxin analyses of shellfish samples conducted throughout the investigated period confirmed that the concentration of toxins was always below the limit of detection (LOD=0.1025 µg DA g^{-1}). Low levels of domoic acid have been reported in shellfish tissue and plankton net samples from this area but in the winter period (Ujević *et al*., 2010; Arapov *et al*., 2016).

Distribution of Pseudo-nitzschia spp. *in relation to environmental parameters*

The bloom that occurred in the Krka River estuary was almost monospecific, involving *P.* cf. *arenysensis* (94%). The period with increased abundance lasted for one month. In the Mediterranean Sea, no *P. arenysensis* bloom has been recorded to date although this species has been originally described from the NW Mediterranean (Quijano-Schegia *et al*., 2009) and later confirmed in Greek coastal waters (Moschandreou *et al*., 2012), the NW Adriatic Sea (Penna

et al., 2013; Pugliese *et al*., 2017) and the Gulf of Naples (Quijano-Schegia *et al*., 2010).

In this study, the highest abundance of *Pseudo-nitzschia* spp. and its ratio in the diatom community was found in a less variable layer, below the halocline. Statistical analyses (PCA and Spearman rank correlation) indicated that *Pseudo-nitzschia* spp. abundance was positively correlated with salinity and orthophosphate concentrations but negatively correlated with nitrates and orthosilicate concentrations. In the Krka River estuary, concentrations of nitrates and orthosilicates are mainly related to river inflow (Cetinić *et al*., 2006) as confirmed by a negative correlation with salinity.

Surface salinity was highly variable throughout the investigated period, but generally low due to increased river inflow (DHMZ, 2019). The highest abundance of *Pseudo-nitzschia* was found with higher salinities, at 7 m sampling depth. We believe that the distribution of *Pseudo-nitzschia* is strongly affected by salinity. A recent study by Ninčević Gladan *et al.* (2020) notes the highest abundance of *Pseudo-nitzschia* spp. in this area during the weakest halocline period. *Pseudo-nitzschia* species are considered as euryhaline species, occurring over a broad salinity range, but some studies have shown that better growth is obtained with higher salinities values (Thessen *et al*., 2005; Lelong *et al*., 2012). In agreement with our results, *Pseudo-nitzschia* species were positively associated with salinity in the studies of Caroppo *et al*. (2005) and Sahraoui *et al*. (2009). Regarding other environmental parameters, *Pseudo-nitzschia* was negatively correlated with nitrate and orthosilicate concentrations as observed in the southwestern Mediterranean (Sahraoui *et al*., 2012). In contrast, Quijano-Scheggia *et al*. (2008a; 2008b) found that high abundances of *P. delicatissima* were associated with a high concentration of nitrates while according to Macintyre *et al*. (2011) submarine groundwaters, rich in nitrate, are potential hot-spots for *Pseudo-nitzschia* blooms.

In this study, the peak of *Pseudo-nitzschia* spp. abundance coincided with the minimum value of Si:TIN ratio (0.34). At that time, the highest nitrate and the lowest orthosilicate concentrations were recorded for a layer at 7 m depth. We assume that in our study, the low Si:TIN ratio was a consequence of decreased orthosilicates concentration due to nutrient uptake for cell growth during the bloom and that nitrates were available for *Pseudo-nitzschia* development. A low Si:N ratio has been previously associated with *Pseudo-nitzschia* blooms in the Adriatic Sea and worldwide (Burić *et al*., 2008; Ljubešić *et al*., 2011; Thorel *et al*., 2017).

Furthermore, the intense proliferation of *Pseudo-nitzschia* spp. observed in our study may have been triggered by an increased concentration of ammonium and orthophosphates that characterised the pre-bloom period. Loureiro *et al*. (2009) showed that *P. delicatissima* successfully utilise ammonia and urea as a source of nitrogen for growth. Similar results were obtained for *P. multiseries*, which grow equally well on different N substrates: nitrates, ammonium, and urea (Radan & Cochlan, 2018). According to Klein *et al*. (2010) a sudden increase of nutrients, $PO4^{3-}$ in particular, may promote the development of *Pseudo-nitzschia* blooms. A positive correlation of *Pseudo-nitzschia* abundance with phosphates concentration was found in several studies (Burić *et al*., 2008; Bosak *et al*., 2009; Ljubešić *et al*., 2011; Trainer *et al*., 2012; Ninčević-Gladan *et al*., 2015). The above results and our findings indicate that not only the availably of nutrients, but also the variation in their ratio can stimulate and cause a bloom of different *Pseudo-nitzschia* species.

Regarding the short sampling period in which seven *Pseudo-nitzschia* species were morphologically determined, the Krka river estuary can be characterised as a highly diverse and suitable environment for the development of *Pseudo-nitzschia* blooms.

Conclusion

Intense proliferation of *Pseudo-nitzschia* species occurred in a middle Adriatic estuary, an important aquaculture area. Morphological and phylogenetic analyses identified *P.* cf. *arenysensis* as the bloom-forming species but despite its high abundance no shellfish toxicity was recorded. In this highly variable environment, salinity was recognised as an important environmental factor affecting the vertical distribution of *Pseudo-nitzschia* species. The availability of the increased ammonium and orthophosphate concentrations, and the low Si:TIN ratio may have stimulated the bloom of *P*. cf. *arenysensis.* We believe that our results present valuable in-situ data on the distribution of this highly diverse diatom genus.

Acknowledgements

Special thanks are due to Mr. Roman Garber for his valuable assistance in field sampling and Mr. Ivan Pezo who performed the nutrient analyses. We greatly appreciate the suggestions of anonymous reviewers who improved our manuscript significantly. This study was fully funded by the Croatian Science Foundation under project IP-2014-09-3606 "Marine plankton as a tool for assessment of climate and anthropogenic influence on the marine ecosystem, MARIPLAN".

References

Adachi, M., Sako, Y., Ishida, Y., 1994. Restriction fragment length polymorphism of ribosomal DNA internal transcribed spacer and 5.8S regions in Japanese *Alexandrium* species (Dinophyceae). *Journal of Phycology*, 30, 857-863.

Ajani, P., Murray, S., Hallegraeff, G., Lundholm, N., Gillings, M. *et al.*, 2013. The diatom genus *Pseudo-nitzschia* (Bacillariophyceae) in New South Wales, Australia: morphology, molecular phylogeny, and distribution. *Journal of Phycology*, 49, 765-785.

Ajani, P.A.,Verma, A., Lassudrie, M., Doblin, M.A., Murray, S.A., 2018. A new diatom species *P. hallegraeffii* sp. nov. belonging to the toxic genus *Pseudo-nitzschia* (Bacillario-

phyceae) from the East Australian Current. *PLos ONE*, 13, e0195622.

Arapov, J., Ujević, I., Marić Pfannkuchen, D., Godrijan, J., Bakrač, A. *et al.*, 2016. Domoic acid in phytoplankton net samples and shellfish from the Krka River estuary in the Central Adriatic Sea. *Mediterranean Marine Science*, 17, 340-350.

Arapov, J., Skejić, S., Bužančić, M., Bakrač, A., Vidjak, O. *et al.*, 2017. Taxonomical diversity of *Pseudo-nitzschia* from the Central Adriatic Sea. *Phycological Research*, 65, 280-290.

Bates, S.S., Hubbard, K.A., Lundholm, N., Montresor, M., Leaw, C.P., 2018. *Pseudo-nitzschia*, *Nitzschia*, and domoic acid: New research since 2011. *Harmful Algae*, 79, 3-43.

Bosak, S., Burić, Z., Djakovac, T., Viličić, D., 2009. Seasonal distribution of plankton diatoms in Lim Bay, northeastern Adriatic Sea. *Acta Botanica Croatica*, 68, 351-365.

Burić, Z., Viličić, D., Caput Mihelić, K., Carić, M., Kralj, K. *et al.*, 2008. *Pseudo-nitzschia* blooms in the Zrmanja River estuary. *Diatom Research*, 23, 51-63.

Bužančić, M., Ninčević Gladan, Ž., Marasović, I., Kušpilić, G., Grbec, B. *et al.*, 2012. Population structure and abundance of phytoplankton in three bays on the eastern Adriatic coast: Šibenik Bay, Kaštela Bay and Mali Ston Bay. *Acta Adriatica*, 53, 413-435.

Caroppo, C., Congestri, R., Bracchini, L., Albertano, P., 2005. On the presence of *Pseudo-nitzschia calliantha* Lundholm, Moestrup et Hasle and *Pseudo-nitzschia delicatissima* (Clave) Heiden in the Southern Adriatic Sea (Mediterranean Sea, Italy). *Journal of Plankton Research*, 27, 763-774.

Cetinić, I., Viličić, D., Burić, Z., Olujić, G., 2006. Phytoplankton seasonality in a highly stratified karstic estuary (Krka, Adriatic Sea). *Hydrobiologia*, 555, 31-40.

Ciminiello, P., Dell'Aversano, C., Fattorusso, E., Forino, M., Magno, G. S. *et al.*, 2005. Hydrophilic interaction liquid chromatography/mass spectrometry for determination of domoic acid in Adriatic shellfish. *Rapid Communications in Mass Spectrometry*, 19, 2030-2038.

Clarke, K.R., Warwick, R.M., 2001. Changes in marine communities: an approach to statistical analysis and interpretation, 2nd edition. PRIMER-E: Plymouth.

DHMZ, 2019. Croatian Meteorological and Hydrological Services. http://hidro.dhz.hr/ (Accessed 12 March 2019)

EU, 2004. Regulation (EC) No 853/2004 of the European Parliament and of the Council of 29 April 2004 laying down specific hygiene rules for food of animal origin. *Official Journal of the European Union* L139, 22-82.

Grasshoff, K., Kremling, K., Ehrhardt, M., 1999. Methods of Seawater Analysis, third ed. Wiley-VCH, Weinheim, 419 pp.

Grbin, D., Pfannkuchen, M, Babić, I., Mejdandžić, M., Mihanović, H. *et al.*, 2017. Multigene phylogeny and morphology of newly isolated strain of *Pseudo-nitzschia mannii* Amato & Montresor (Adriatic Sea). *Diatom Research*, 32, 127-131.

Hansen, L.R., Soylu, S., Kotaki, Y., Moestrup, Ø., Lundholm, N., 2011. Toxin production and temperature-induced morphological variation of the diatom *Pseudo-nitzschia seriata* from the Arctic. *Harmful Algae*, 10, 689-696.

Hasle, G.R., Fryxell, G.A., 1970. Diatoms: Cleaning and mounting for light and electron microscopy. *Transactions of the American Microscopical Society*, 89, 469-474.

Huang C.X., Dong, H.C., Lundholm, N., Teng, S.T., Zheng, G.C. *et al.*, 2019. Species composition and toxicity of the genus *Pseudo-nitzschia* in Taiwan Strait, including *P. chiniana* sp. nov. and *P. qiana* sp. nov. *Harmful Algae*, 84, 195-209.

Kearse, M., Moir, R., Wilson, A., Stones-Havas, S., Cheung, M. *et al.*, 2012. Geneious Basic: An integrated and extendable desktop software platform for the organization and analysis of sequence data. *Bioinformatics*, 28, 1647-1649.

Klein, C., Claquin, P., Bouchart, V., Le Roy, B., Véron, B., 2010. Dynamics of *Pseudo-nitzschia* spp. and domoic acid production in a macrotidal ecosystem of the Eastern English Channel (Normandy, France). *Harmful Algae*, 9, 218-226.

Kumar, S., Stecher, G., Tamura, K., 2016. MEGA7: Molecular Evolutionary Genetics Analysis Version 7.0 for Big- ger Datasets. *Molecular Biology and Evolution*, 33, 1870-1874.

La Barre, S., Bates, S.S., Quilliam, M.A., 2014. Domoic Acid. p. 189-215. In: *Outstanding Marine Molecules: Chemistry, Biology, Analyses*. La Barre, S., Kornprobost, J.-M. (Eds.). Wiley-VCH Verlag GmbH & Co. KGaA.

Lelong, A., Hégaret, H., Soudant, P., Bates S.S., 2012. *Pseudo-nitzschia* (Bacillariophyceae) species, domoic acid and amnesic shellfish poisoning: revisiting previous paradigms. *Phycologia*, 51, 168-216.

Lim, H.C., Teng, S.T., Leaw, C.P., Lim, P.T., 2013. Three novel species in the *Pseudo-nitzschia pseudodelicatissima* complex: *P. batesiana* sp. nov., *P. lundholmiae* sp. nov., and *P. fukuyoi* sp. nov. (Bacillariophyceae) from the strait of Malacca, Malaysia. *Journal of Phycology*, 49, 902-916.

Loureiro, S., Jauzein, C., Garcés, E., Collos, Y., Camp, J. *et al.*, 2009. The significance of organic nutrients in the nutrition of *Pseudo-nitzschia delicatissima* (Bacillaeriophyceae). *Journal of Plankton Research*, 31, 399-410.

Lundholm, N. (Ed), 2019. Bacillariophyceae, in IOC-UNESCO Taxonomic Reference List of Harmful Micro Algae. Available online at http://www.marinespecies.org/hab (Accessed 24 September 2019).

Lundholm, N., Moestrup, Ø., Kotaki, Y., Hoef-Emden, K., Scholin, C. *et al.*, 2006. Inter- and intraspecific variation of the *Pseudo-nitzschia delicatissima* complex (Bacillariophyceae) illustrated by rRNA probes, morphological data and phylogenetic analyses. *Journal of Phycology*, 42, 464-481.

Ljubešić, Z., Bosak, S., Viličić, D., Kralj Borojević, K., Marić, D. *et al.*, 2011. Ecology and taxonomy of potentially toxic *Pseudo-nitzschia* species in Lim Bay (north-eastern Adriatic Sea). *Harmful Algae*, 10, 713-722.

Macintyre, H.L., Stutes, A.L., Smith, W.L., Dorsey, C.P., Abraham, A. *et al.*, 2011. Environmental correlates of community composition and toxicity during a bloom of *Pseudo-nitzschia* spp. in the Northern Gulf of Mexico. *Journal of Plankton Research*, 33, 273–295.

Marchetti, A., Harrison, P.J., 2007. Coupled changes in the cell morphology and the elemental (C, N, and Si) composition of the pennate diatom *Pseudo-nitzschia* due to iron deficiency. *Limnology and Oceanography*, 52 (5), 2270-2284.

Marchetti, A., Lundholm, N., Kotaki, Y., Hubbard, K., Harrison, P. J. *et al.*, 2008. Identification and assessment of domoic acid production in oceanic *Pseudo-nitzschia* (Bacillariophyceae) from iron-limited waters in the northeast subarctic Pacific. *Journal of Phycology*, 44, 650-61.

Marić Pfannkuchen, D. 2013. Potentially toxic diatom genus *Pseudo-nitzschia* in the northern Adriatic Sea: ecological, taxonomic and molecular features. Ph.D. Thesis, University of Zagreb, Zagreb, Croatia, 195 pp.

Marić, D., Ljubešić, Z., Godrijan, J., Viličić, D., Ujević, I. *et al.*, 2011. Blooms of the potentially toxic diatom *Pseudo-nitzschia calliantha* Lundholm, Moestrup & Hasle in coastal waters of the northern Adriatic Sea (Croatia). *Estuarine, Coastal and Shelf Science*, 92, 323-331.

Marić, D., Kraus, R., Godrijan, J., Supić, N., Djakovec, T. *et al.*, 2012. Phytoplankton response to climatic and anthropogenic influences in the north-eastern Adriatic during the four last decades. *Estuarine, Coastal and Shelf Science*, 115, 98-112.

Montagnes, D.J.S., Franklin, D.J., 2001. Effects of temperature on diatom volume, growth rate, and carbon and nitrogen content: Reconsidering some paradigms. *Limnology and Oceanography*, 46 (8), 2008-2018.

Moschandreou, K.K., Nikolaidis, G., 2010. The genus *Pseudo-nitzschia* (Bacillariophyceae) in Greek coastal waters. *Botanica Marina*, 53, 159-172.

Moschandreou, K.K., Baxevanis, A.D., Katikou, P., Papaefthimiou, D., Nikolaidis, G. *et al.*, 2012. Inter- and intra-specific diversity of *Pseudo-nitzschia* (Bacillariophyceae) in the northeastern Mediterranean. *European Journal of Phycology*, 47, 321-339.

Ninčević-Gladan, Ž., Bužančić, M., Kušpilić, G., Grbec, B., Matijević, S. *et al.*, 2015. The response of phytoplankton community to anthropogenic pressure gradient in the coastal waters of the eastern Adriatic Sea. *Ecological Indicators*, 56, 106-115.

Ninčević Gladan, Ž., Matić, F., Arapov, J., Skejić, S., Bužančić, M. *et al*., 2020. The relationship between toxic phytoplankton species occurrence and environmental and meteorological factors along the Eastern Adriatic coast. *Harmful Algae*, 92, doi.org/10.1016/j.hal.2020.101745.

Orive, E., Pérez-Aicuna, L., David, H., García-Etxebarria, K., Laza-Martínez, A. *et al.*, 2013. The genus *Pseudo-nitzschia* (Bacillariophyceae) in a temperate estuary with description of two new species: *Pseudo-nitzschia plurisecta* sp. nov. and *Pseudo-nitzschia abrensis* sp. nov. *Journal of Phycology*, 49, 1192-1206.

Orlova, T.Y., Stonik, I.V., Aizdaicher, N.A., Bates, S.S., Léger, C. *et al.*, 2008. Toxicity, morphology and distribution of *Pseudo-nitzschia calliantha*, *P. multistriata* and *P. multiseries* (Bacillariophyta) from the northwestern Sea of Japan. *Botanica Marina*, 51, 297-306.

Orsini, L., Sarno, D, Procaccini, G., Poletti, R., Dahlmann, J. *et al.*, 2002. Toxic *Pseudo-nitzschia multistriata* (Bacillariophyceae) from the Gulf of Naples: morphology, toxin analyses and phylogenetic relationships with other *Pseudo-nitzschia* species. *European Journal of Phycology*, 37, 247-257.

Penna, A., Casabianca, S., Perini, F., Bastianini, M., Riccardi, E. *et al.*, 2013. Toxic *Pseudo-nitzschia* spp. in the northwestern Adriatic Sea: characterization of species composition by genetic and molecular quantitative analyses. *Journal of Plankton Research*, 35, 352-366.

Pistocchi, R., Guerrini, F., Pezzolesi, L., Riccardi, M., Vanucci, S. *et al.*, 2012. Toxin levels and profiles in microalgae from the North-western Adriatic Sea- 15 years of studies on cultured species. *Marine Drugs*, 10, 140-162.

Pugliese, L., Casabianca, S., Perini, F., Andreoni, F., Penna, A., 2017. A high resolution melting method for the molecular identification of the potentially toxic diatom *Pseudo-nitzschia* spp. in the Mediterranean Sea. *Scientific Reports*, 7, 4259.

Quijano-Scheggia, S., Garcés, E., Flo, E., Fernandez-Tejedor, M., Diogene, J. *et al.*, 2008a. Bloom dynamics of the genus *Pseudo-nitzschia* (Bacillariophyceae) in two coastal bays (NW Mediterranean Sea). *Scientia Marina*, 72, 577-590.

Quijano-Scheggia, S., Garcés, E., Sampedro, N., Van Lenning, K., Flo, E. *et al.*, 2008b. Identification and characterisation of the dominant *Pseudo-nitzschia* species (Bacillariophyceae) along the NE Spanish coast (Catalonia, NW Mediterranean). *Scientia Marina*, 72, 343-359.

Quijano-Scheggia, S., Garcés, E., Lundholm, N., Moestrup, Ø, Andree, K. *et al.*, 2009. Morphology, physiology, molecular phylogeny and sexual compatibility of the cryptic *Pseudo-nitzschia delicatissima* complex (Bacillariophyta), including the description of *P. arenysensis* sp. nov. *Phycologia*, 48, 492-509.

Quijano-Scheggia, S., Garcés, E., Andree, K.B., Iglesia, P., Diogène, J. *et al.*, 2010. *Pseudo-nitzschia* species on the Catalan coast: charcterization and contribution to the current knowledge of the distribution of this genus in the Mediterranean Sea. *Scientia Marina,* 74, 395-410.

Quilliam, M. A., Xie, M., Hardstaff, W. R., 1995. A rapid extraction and cleanup procedure for the liquid chromatographic determination of domoic acid in unsalted seafood. *Journal of AOAC International*, 78, 543-554.

Radan, R.L., Cochlan, W.P., 2018. Differential toxin response of *Pseudo-nitzschia multiseries* as a function of nitrogen speciation in batch and continuous cultures, and during a natural assemblage experiment. *Harmful Algae*, 73, 12-29.

Rivera-Vilarelle, M., Quijano-Scheggia, S., Olivos-Ortiz, A., Gaviño-Rodríguez, J.H., Castro-Pchoa, F. *et al.*, 2013. The genus *Pseudo-nitzschia* (Bacillariophyceae) in Manzanillo and Santiago Bays, Colima, Mexico. *Botanica Marina*, 56, 357-373.

Ronquist, F., Huelsenbeck, J.P., 2003. MrBayes 3: Bayesian phylogenetic inference under mixed models. *Bioinformatics*, 19, 1572-1574.

Sahraoui, I., Hlaili, A.S., Mabrouk, H.H., Léger, C., Bates, S.S., 2009. Blooms of the diatom genus *Pseudo-nitzschia* H. Pergallo in Bizerte lagoon (Tunisia, SW Mediterranean). *Diatom Research*, 24, 175-190.

Sahraoui, I., Bates, S. S., Bouchouicha, D., Mabrouk, H. H., Hlaili, A.S., 2011. Toxicity of *Pseudo-nitzschia* population from Bizerte Lagoon, Tunisia, southwest Mediterranean, and first report of domoic acid production by *P. brasiliana*. *Diatom Research*, 26, 293-303.

Sahraoui, I., Grami, B., Bates, S.S., Bouchouicha, D., Chikhaoui, M.A. *et al.*, 2012. Response of potentially toxic *Pseudo-nitzschia* (Bacillariophyceae) population and domoic acid to environmental conditions in a eutrophied, SW Mediterranean coastal lagoon (Tunisia). *Estuarine, Coastal and Shelf Science*, 102-103, 95-104.

Schlitzer, R., Ocean Data View, https://odv.awi.de, 2018.

Scholin, C.A., Herzog, M., Sogin, M., Anderson, D.M., 1994. Identification of group and strain-specific using genetic

markers from globally distributed *Alexandrium* (Dinophyceae). II. Sequence analysis of fragments of the LSU rRNA gene. *Journal of Phycology*, 999-1011.

Skejić, S., Bojanić, N, Matijević, S., Vidjak, O., Grbec, B. *et al.*, 2014. Analysis of the phytoplankton community in the vicinity of domestic sewage outflow during stratified conditions. *Mediterranean Marine Science*, 15, 574-586.

Stonik, I.V., Orlova, T.Y., Lundholm, N., 2011. Diversity of *Pseudo-nitzschia* H. Peragallo from the western North Pacific. *Diatom Research*, 26, 121-134.

Stonik, I.V., Isaeva, M.P., Aizdaicher, N.A., Balakirev, E.S., Ayala, F.J., 2018. Morphological and genetic identification of *Pseudo-nitzschia* H. Peragallo, 1900 (Bacillariophyta) from the Sea of Japan. *Russian Journal of Marine Biology*, 44, 192-201.

Su, Y., Lundholm, N., Ellegaard, M., 2018. Effects of abiotic factors on the nanostructure of diatom frustules-ranges and variability. *Applied Microbiology and Biotechnology*, 102, 5889-5899.

Svensen, C., Viličić, D., Wassmann, P., Arashkevich, E., Ratkova, T., 2007. Plankton distribution and vertical flux of biogenic matter during high summer stratification in the Krka river estuary (Eastern Adriatic). *Estuarine, Coastal and Shelf Science*, 71, 381-390.

Teng, S.T., Leaw, C.P., Lim, H.C., Lim, P.T., 2013. The genus *Pseudo-nitzschia* (Bacillariophyceae) in Malaysia, including new records and a key to species inferred from morphology-based phylogeny. *Botanica Marina*, 56, 375-398.

Teng, S.T., Tan, S.N., Lim, H.C., Dao, V.H., Bates, S.S. *et al.*, 2016. High diversity of *Pseudo-nitzschia* along the northern coast of Sarawak (Malaysian Borneo), with descriptions of *P. bipertita* sp. nov. and *P. limii* sp. nov. (Bacillariophyceae). *Journal of Phycology*, 49, 973-989.

Thessen, A.E., Dortch, Q., Parsons, M.L., Morrison, W., 2005. Effect of salinity on *Pseudo-nitzschia* species (Bacillariophyceae) growth and distribution. *Journal of Phycology*, 41, 21-29.

Thorel, M., Claquin, P., Schapira, M., Le Gendre, R., Riou, P. *et al.*, 2017. Nutrient ratios influence variability in *Pseudo-nitzschia* species diversity and particulate domoic acid production in the Bay of Seine (France). *Harmful Algae*, 68, 192-205.

Trainer, V.L., Bates, S.S., Lundholm, N., Thessen, A.E., Cochlan, W.P. *et al.*, 2012. *Pseudo-nitzschia* physiological ecology, phylogeny, toxicity, monitoring and impacts on ecosystem health. *Harmful Algae*, 14, 271-300.

Turk Dermastia, T., Cerino, F., Stanković, D., Francé, J., Ramšak, A. *et al.* 2020. Ecological time series and integrative taxonomy unveil seasonality and diversity of the toxic diatom *Pseudo-nitzschia* H. Pergallo in the northern Adiratic Sea. *Harmful Algae*, 93.

Ujević, I., Ninčević Gladan, Ž., Roje, R., Skejić, S., Arapov, J. *et al.*, 2010. Domoic acid – A New Toxin in the Croatian Adriatic Shellfish Toxin Profile. *Molecules*, 15, 6835-6849.

Utermöhl, H., 1958. Zur Vervollkommung der quantitative Phytoplankton Methodik. *Internationale Vereinigung für Theoretische und angewandte Limnologie*, 9, 1-38.

Viličić, D., Legović, T., Žutić, V., 1989. Vertical distribution of phytoplankton in a stratified estuary. *Aquatic Sceinces*, 51 (1), 31-46.

Viličić, D., Bosak, S., Burić. Z., Caput-Mihalić, K., 2007. Phytoplankton seasonality and composition along the coastal NE Adriatic Sea during the extremely low Po River discharge in 2006. *Acta Botanica Croatica*, 66, 101-115.

Viličić, D., Djakovac, T., Burić, Z., Bosak, S. 2009. Composition and annual cycle of phytoplankton assemblages in the northeastern Adriatic Sea. *Botanica Marina*, 52, 291-305.

Wright, J.L.C., Boyd, R. K., De Freitas, A.S.W., Falk, M., Foxall, R.A. *et al.*, 1989. Identification of domoic acid, a neuroexcitatory amino acid, in toxic mussels from eastern Prince Edward Island. *Canadian Journal of Chemistry*, 67, 481-490.